View metadata, citation and similar papers at core.ac.uk

brought to you by CORE

provided by Archive Ouverte en Sciences de l'Information et de la Communication

Black box EMC modeling of a three phase inverter

Meriem Amara, Christian Vollaire, Marwan Ali, François Costa

To cite this version:

Meriem Amara, Christian Vollaire, Marwan Ali, François Costa. Black box EMC modeling of a three phase inverter. EMC Europe, Aug 2018, Amsterdam, Netherlands. 10.1109/EMCEurope.2018.8485007 . hal-02051465

HAL Id: hal-02051465

https://hal.archives-ouvertes.fr/hal-02051465

Submitted on 27 Feb 2019

HAL is a multi-disciplinary open access archive for the deposit and dissemination of scientific research documents, whether they are published or not. The documents may come from teaching and research institutions in France or abroad, or from public or private research centers.

L'archive ouverte pluridisciplinaire **HAL**, est destinée au dépôt et à la diffusion de documents scientifiques de niveau recherche, publiés ou non, émanant des établissements d'enseignement et de recherche français ou étrangers, des laboratoires publics ou privés.

Black box EMC modeling of a three phase inverter

Meriem Amara, Christian Vollaire
Ecole Centrale de Lyon
Ampère-CNRS
Lyon, France
Email: meriem.amara@doctorant.ec-lyon.fr

Marwan Ali
Safran
Paris, France

Francois Costa
Université Paris Est Créteil
SATIE CNRS
Cachan, France

***Abstract*—This paper presents an Electromagnetic Interferences (EMI) modeling of a DC-AC power converter, based on a black box representation: the converter is represented by an association of sources and impedances that reflect its external EMI behavior. This modeling approach presented in this paper requires a very short computation time, which allows an optimized design of an EMC filter or an interaction study between several converters connected on the same electrical network. This EMC model depending on a given operation point of the converter, the second part of this paper is dedicated to the study of the load influence on this behavioral model.**

Keywords— power electronic converters, electromagnetic compatibility, EM modeling, EMC filter

I. INTRODUCTION

Nowadays, the use of power converters in systems "more electric" (actuation, pumping, conversion, lighting, etc.) requires to control conducted emissions. The electromagnetic compatibility (EMC) of any equipment in its environment avoids any risk of interference, or alteration of the functional performance of sensitive systems.

Thanks to the progress of power electronics, and in order to gain mass on the distribution of electrical energy, more and more aircraft manufacturers are planning to migrate to a high-voltage DC distribution (HVDC). With the voltage rise, dv/dt have a greater impact on conducted emissions compared to what is currently known. In addition, the use of higher switching frequencies in high power converters enabled by wide bandgap semiconductors constitutes a major electromagnetic risk that must be controlled. In order to protect the networks and loads from these emissions, and to meet the standards for electromagnetic compatibility (EMC) including the aeronautic standard "DO160F", EMC filters are absolutely necessary [1],[2].

An efficient and optimized EMC filter requires a specific design for the two modes of propagation of parasitic currents, i.e., Common Mode (CM) and Differential Mode (DM). The design is based on the use of an accurate EMI model of the converter. Behavioral model has proved its efficiency in representing accurately electromagnetic interferences [3], [4]. This kind of model is constituted by disturbance equivalent sources associated to CM and DM equivalent impedances [5].

In the following paragraphs, we will present the application of this method on a three-phase inverter. Then, an experimental validation will be presented including a study of the impact of the operating point on the generated EMI and thus on the model.

II. EM MODELING OF AN INVERTER

The system under test has two access ports and a ground port on the network side. In the context of this study, we aim to represent accurately electromagnetic interferences of an existing converter, considered from the DC network, owing to an experimental procedure and without knowledge of the internal electrical architecture. In this EMC modeling approach, a Z_{DM} impedance and an I_{DM} source are placed between the two input lines to represent the differential mode (DM) model. The CM one is represented by two identical Z_{CM} impedances connected to a voltage source V_{CM} placed between each of the lines and the ground (Fig. 1).

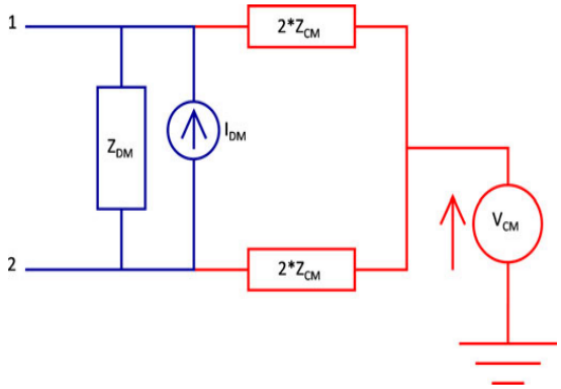

Fig. 1. Global converter EMC model

This EMC model can be identified, using a simple measurement protocol based on the separation of propagation modes, in order to allow the optimized design of two filtering structures (CM and DM) dedicated to each mode of disturbance. The support of our study is a 4 kW drive chain including a DC / AC converter (MOSFET based) feeding an RL load that emulates an electric actuator.

A. Impedance Modeling

The equipment under test is modeled as seen from the network side. It has two ports and a ground connection. Therefore, the impedance matrix can be calculated as follows:

$$[V] = [Z][I] \Rightarrow \begin{bmatrix} V_1 \\ V_2 \end{bmatrix} = \begin{bmatrix} Z_{11} & Z_{12} \\ Z_{21} & Z_{22} \end{bmatrix} \begin{bmatrix} I_1 \\ I_2 \end{bmatrix} \quad (1)$$

The indices in (1) correspond to the access numbers in Fig. 1. The relations allowing to compute the CM and DM sources from voltages and currents in structure are:

$$V_{CM} = \frac{V_1+V_2}{2};\ V_{DM} = V_1 - V_2 \quad (2)$$

$$i_{CM} = I_1 + I_2;\ i_{DM} = \frac{I_1-I_2}{2} \quad (3)$$

$$\begin{bmatrix} V_{CM} \\ V_{DM} \end{bmatrix} = \begin{bmatrix} 1/2 & 1/2 \\ 1 & -1 \end{bmatrix} \begin{bmatrix} V_1 \\ V_2 \end{bmatrix} \quad (4)$$

$$\begin{bmatrix} I_1 \\ I_2 \end{bmatrix} = \begin{bmatrix} 1/2 & 1 \\ 1/2 & -1 \end{bmatrix} \begin{bmatrix} i_{CM} \\ i_{DM} \end{bmatrix} \quad (5)$$

$$=> \begin{bmatrix} V_{CM} \\ V_{DM} \end{bmatrix} = [P][Z][P]^t \begin{bmatrix} i_{CM} \\ i_{DM} \end{bmatrix} \text{ Avec } P = \begin{bmatrix} 1/2 & 1/2 \\ 1 & -1 \end{bmatrix} \quad (6)$$

$$=> \begin{bmatrix} V_{CM} \\ V_{DM} \end{bmatrix} = \begin{bmatrix} \frac{Z_{11}+Z_{12}+Z_{21}+Z_{22}}{4} & \frac{Z_{11}-Z_{12}+Z_{21}-Z_{22}}{2} \\ \frac{Z_{11}+Z_{12}-Z_{21}-Z_{22}}{2} & Z_{11}-Z_{12}-Z_{21}+Z_{22} \end{bmatrix} \begin{bmatrix} i_{CM} \\ i_{DM} \end{bmatrix} \quad (7)$$

$$=> \begin{bmatrix} V_{CM} \\ V_{DM} \end{bmatrix} = \begin{bmatrix} Z_{CM} & Z'_{conversion} \\ Z_{conversion} & Z_{DM} \end{bmatrix} \begin{bmatrix} i_{CM} \\ i_{DM} \end{bmatrix} \quad (8)$$

In our case, four impedances are measured directly with an impedance analyzer when the converter is off and connected to the load. The procedure is as follows:

- Z_{11} is measured between line 1 and ground,
- Z_{22} is measured between line 2 and ground,
- Z_{CM} is measured between the two short-circuited lines on one side and the ground on the other side,
- Z_{DM} is measured between line 1 and line 2 (converter placed far from the ground).

This modules of impedances are shown in Fig. 2:

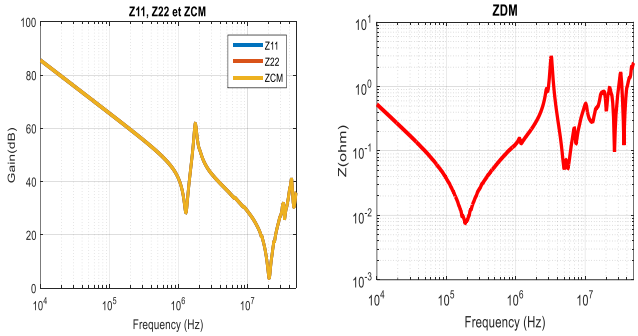

Fig. 2. Measured input impedances

From these measurements, the impedances Z_{11} and Z_{22} are clearly identical leading to the same CM impedance. This allows us to propose a simple electrical model with only three localized impedances (see in Fig. 3).

The proposed model consists of two parallel RLC circuits placed between each line and the ground.

The DM impedance is also represented by two parallel RLC circuits placed between the two input lines.

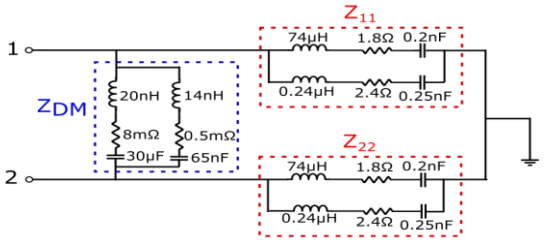

Fig. 3. Converter equivalent model of impedance for EMI analysis

Measurements and identifications led to the determination of the value of each element of the model [6]. These values are shown in Fig. 3.The theoretical impedances corresponding to each measurement configuration have been calculated from this model.

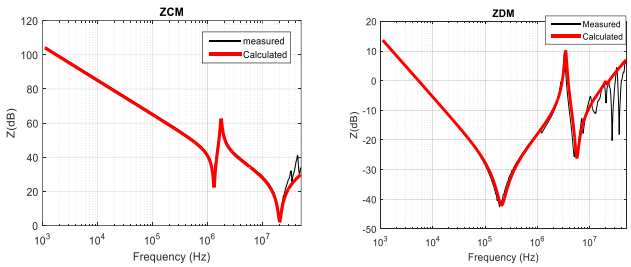

Fig. 4. Comparison between measured and calculated input impedances

The experimental results presented in Fig. 4 are clearly in good agreement with simulated results up to 30 MHz.

B. CM and DM Sources Model

The EMC model must be completed by two equivalent CM and DM sources. The symmetry of the line impedances limits the phenomena of mode conversion, which simplifies the extraction of the equivalent sources.

In order to realize this extraction, the power converter is fed through two identical line impedance stabilization networks (LISN) placed on each line between the network and the system under test. They have two main functions. Firstly, they prevent incoming CM and DM disturbances from the supply network. Secondly, they maintain the specified impedance at the system under test over the working frequency range. This impedance is standardized by DO160F. The equivalent EMC model corresponding to this measurement configuration is shown in **Erreur ! Source du renvoi introuvable.**.

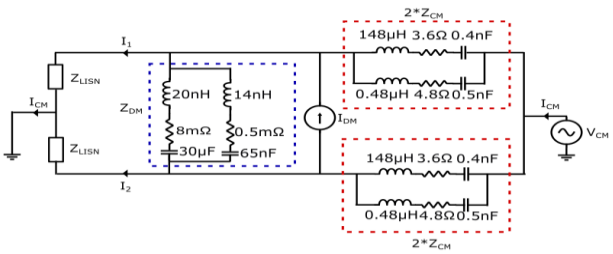

Fig. 5. CM and DM sources associated with the power converter equivalent model of impedance

According to the complete model given in Fig. 1, the equivalent sources can be extracted by measuring the two line currents (between LISNs and the converter). The equivalent CM voltage source and the DM current source can be calculated by:

$$I_1 + I_2 = I_{MC} \Rightarrow V_{MC} = (I_1 + I_2)\left(\frac{Z_{RSIL}+2Z_{MC}}{2}\right) \quad (9)$$

$$I_1 - I_2 = 2\frac{\left(\frac{4Z_{MC}Z_{MD}}{4Z_{MC}+Z_{MD}}\right)I_{MD}}{\left(2Z_{RSIL}+\frac{4Z_{MC}Z_{MD}}{4Z_{MC}+Z_{MD}}\right)}$$

$$\Rightarrow I_{MD} = (I_1 - I_2)\left(\frac{Z_{RSIL}}{4Z_{MC}} + \frac{Z_{RSIL}}{Z_{MD}} + \frac{1}{2}\right) \quad (10)$$

Before measuring the currents I_1+I_2 and I_1-I_2, it is necessary to determine the "black box" model of the LISN. The characterization of the LISN is performed as close as possible to the boxes after adding a 50 ohm in parallel with the resistance R2 of the LISN (see in Fig. 6).

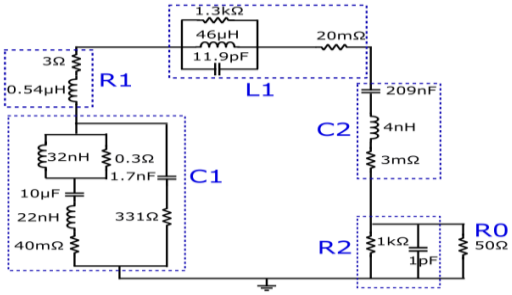

Fig. 6. Equivalent model of the LISN

In order to improve the accuracy in the calculation of the two equivalent sources, currents I_1+I_2 and I_1-I_2 have been directly measured on the test bench using two identical current probes (Pearson Model 6595, 0.25 V/A, 50 Ω) for a given operating point (V_{DC} = 540V et I_{DC} = 3,6A). The acquisitions at this step are performed using an oscilloscope LeCroy (WaveRunner HRO 64 Zi 400 MHz 12bit 2gs/s). The FFT of the time domain measurements are then processed. The frequency domain data are corrected by applying the inverse transfer function of the sensors, leading to the current values, i.e. I_1+I_2 and I_1-I_2. The CM and DM sources are then calculated using (9) and (10). The calculated spectrum corresponding to CM and DM sources are shown in Fig. 8 and Fig. 8.

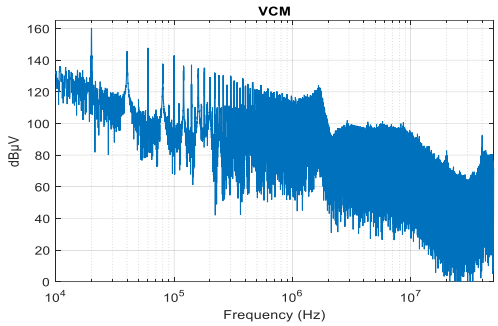

Fig. 7. Calculated spectrum of CM sources (FFT)

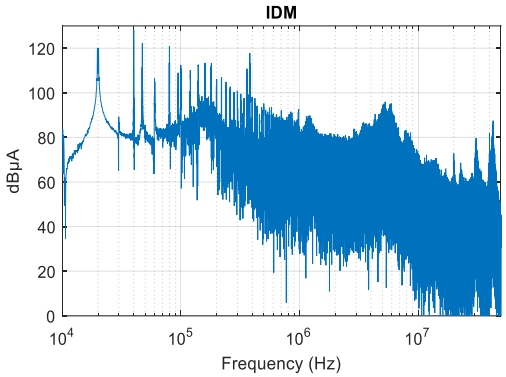

Fig. 8. Calculated spectrum of DM sources (FFT)

C. EMC Model Validation

In order to verify that the proposed model can correctly represent the levels of EMI generated by the converter, we have calculated the LISN voltages from the model shown in **Erreur ! Source du renvoi introuvable.**. Meanwhile, these LISN voltages have been measured directly using the oscilloscope. Experimental and calculated LISN voltage spectrum corresponding to V_{Rlisn1} and V_{Rlisn2} are shown in Fig. 9. We observe a good matching of the two spectra which proves that the proposed model as well as the method of identification of its parameters are correct.

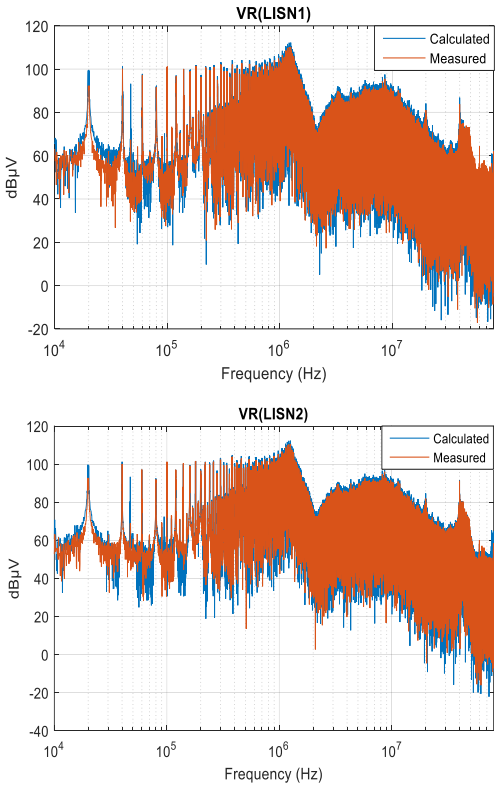

Fig. 9. Calculated and measured LISN voltages

This EMC model, constituted by disturbance equivalent sources and CM and DM equivalent impedances, provides a relevant way to calculate and to optimize the EMC filter for a

given operating point. In the next section, the impact of a change in the operating point on our model will be shown.

III. IMPACT OF THE OPERATING POINT

To be able to change the operating point of the PWM inverter under test, we used a three-phase Star-connected balanced RL load whose resistance is variable. We chose 4 operating points: the first corresponds to 5% of the total power that can dissipate the load that corresponds to 200 W, the second 30% that corresponds to 1.2 kW, the third 60% that corresponds to 2.4 kW and the last 90% that corresponds to 3.6 kW.

The first step consists to observe the influence of different operating points on the impedance measurements. We followed the same procedure described in paragraph II.A to measure the CM and DM impedances for the different points; the following curves have been obtained:

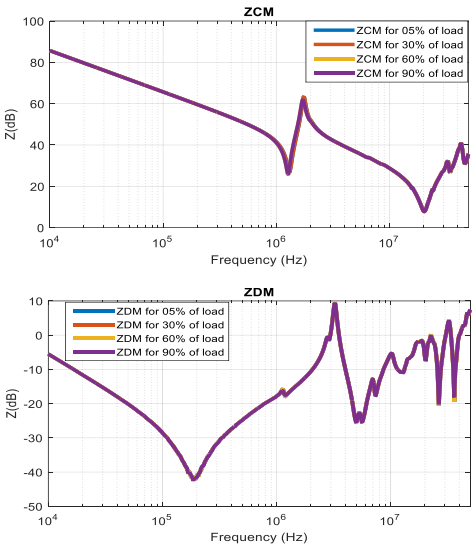

Fig. 10. Measured impedances for four operating points

These measurements show that the variation of the load has no measurable impact on the equivalent DM & CM impedances. These results look to be logical because the physical structure of the system under test has not changed with the operating point. This allows us to maintain the same impedance model presented in Fig. 3 for the different operating points.

The second step consists to observe the impact of the load variation on the current measurements. We followed the same steps as described in Section II.2 to obtain the equivalent CM and DM disturbance sources spectrum; they are shown in Fig. 11 and Fig. 12.

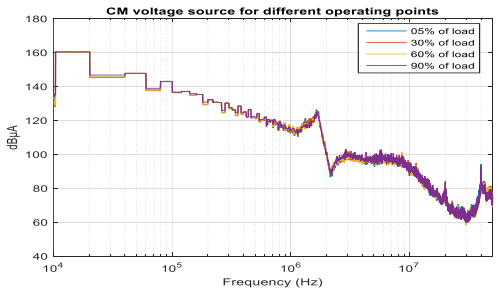

Fig. 11. CM source for different operating points

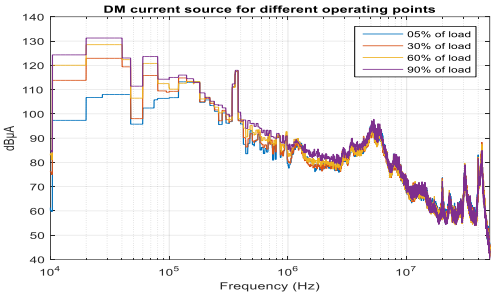

Fig. 12. DM source for different operating points

Considering these spectra, we note that the change of operating point has no impact on the CM source, only the DM one is impacted. These results look to be logical because the CM current mainly depends on the variation of the voltage in the switching cells [7], [8], [9]. The value of this CM current can be evaluated by the equation:

$$I_{CM} = C \frac{dV}{dt} \tag{12}$$

However, the variation of the switching voltage depends mainly on the gate resistance R_G:

$$\frac{dV}{dt} = \frac{V_G - V_{MILLER}}{C_{GD} R_G} \tag{13}$$

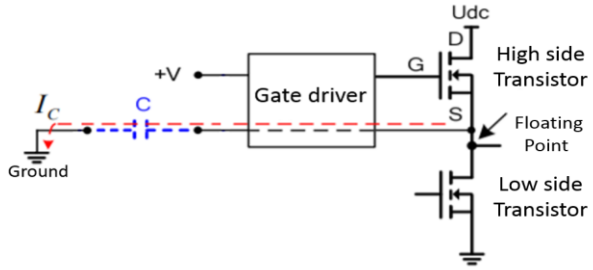

Fig. 13. Electromagnetic disturbance due to the CM [9]

Therefore, a low R_G gate resistance causes fast switching, with higher dv/dt dynamics and, consequently, the CM current is more important. However, a large R_G gate resistance value causes slow switching, with smaller dv/dt dynamics and hence a low CM current [8]. In our case, when we change the operating point of the power converter, we change the power and subsequently the current dissipated by the load. However, the control of the converter (gate resistance, gate voltage) remains the same. Therefore, the CM current does not change significantly.

On the other hand, we observe a difference between the curves of the different operating points from the switching frequency up to 2 MHz for the DM source. These results look to be logical because the DM current mainly depends on the load current and on the diode recovery mechanism [10]. The increase in the load current increases also the maximum recovery current and thus the disturbance levels. The overcurrent propagates in

the network and its influence can be observed in the DM current measured at the network level.

To clearly observe the evolution of the DM current as a function of load variations, we have firstly represented the curves of I_{DM} for which the envelope of the DM source is the largest for three operating points (see Fig. 14). Then, we have represented these curves in 3D to observe the evolution of the DM current according to the frequencies and the variation of load power at the same time (see Fig. 15). Finally, the (Fig. 16) presents the DM current as a function of the load power variation for different frequencies.

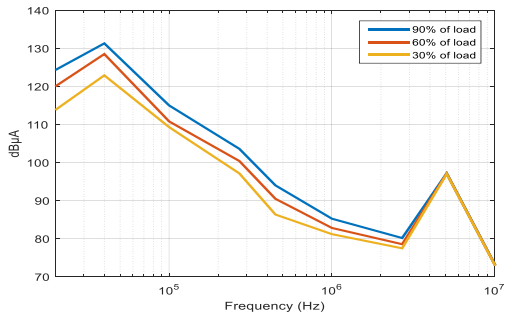

Fig. 14. DM current spectra for different operating points

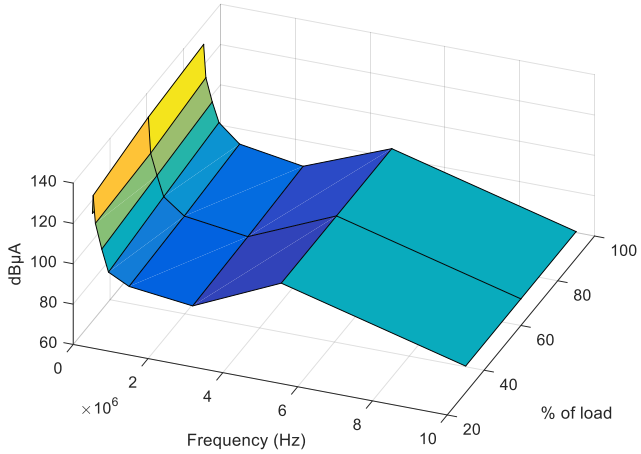

Fig. 15. DM current according to the frequencies and the variation of load power at the same time

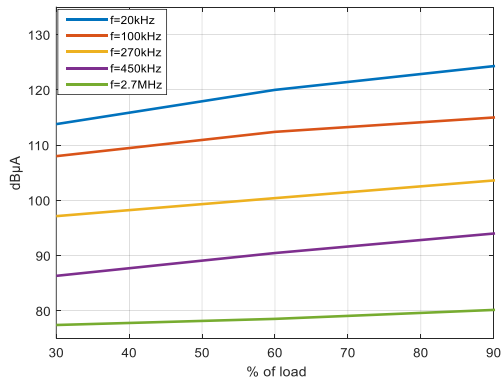

Fig. 16. Evolution of DM current as a function of the load variation for a given frequency

From these curves, we note that the DM current evolves quite linearly with the variation of load power. This type of behavior is very interesting because the evaluation of the DM current in the frequency domain can be done for any operating point even if it has not been identified during the measurements. A few operating points (at least 2) are sufficient to inform the model parameters.

In our case, we have chosen to identify the model in the worst case (the operating point for which the harmonics of the current are maximum) in order to size the filter. Consequently, it will be valid for the other operating points at lower output power. It would be possible to do the same for the modeling of an electrical distribution network (system approach) on which several converters would be connected.

IV. Conclusion

Reducing the volume and improving the efficiency of EMC filters of power equipment are strategic issues, particularly in the case of complex systems such as those found in aerospace or automotive industries. In this paper, a characterization procedure for a DC-AC converter has been presented. Then, a study of the impact of its operating point was carried out, in order to evaluate the evolution of the parameters of the EMC model with the load current.

This method makes it possible to build a behavioral EMC model in the frequency domain of an existing converter. Note that this type of model can be built from an extensive model (predictive), this reduces the runtime of the model.

Acknowledgments

The authors would like to express their thanks to DGAC that funds the project.

References

[1] H. Akagi and T. Shimizu, “Attenuation of Conducted EMI Emissions,” *IEEE Trans. Power Electron.*, vol. 23, no. 1, pp. 282–290, 2008.

[2] K. Raggl, T. Nussbaumer, and J. W. Kolar, “Guideline for a Simplified Differential-Mode EMI Filter Design,” *IEEE Trans. Ind. Electron.*, vol. 57, no. 3, pp. 1031–1040, 2010.

[3] A. C. Baisden, D. Boroyevich, and F. Wang, “Generalized Terminal Modeling of Electromagnetic Interference,” *IEEE Trans. Ind. Appl.*, vol. 46, no. 5, pp. 2068–2079, 2010.

[4] P. Chen and Y. Lai, “Effective EMI Filter Design Method for Three-Phase Inverter Based Upon Software Noise Separation,” *IEEE Trans. Power Electron.*, vol. 25, no. 11, pp. 2797–2806, 2010.

[5] M. Ali, “Nouvelles Architectures intégrées de filtre CEM Hybride,” PhD thesis, ENS Cachan, 2012.

[6] V. Tarateeraseth, S. Member, B. Hu, K. Y. See, S. Member, and F. G. Canavero, “Accurate Extraction of Noise Source Impedance of an SMPS Under Operating Conditions,” *IEEE Trans. Power Electron.*, vol. 25, no. 1, pp. 111–117, 2010.

[7] P.-O. Jeannin, “Le transistor MOSFET en commutation: Application

aux associations série et parallèle de composants à grille isolée .," PhD thesis, INP Grenoble, 2001.

[8] Duc. Ngoc. To, "Circuit de pilotage intégré pour transistor de puissance," PhD thesis, UGA, Grenoble, 2015.

[9] The van Nguyen, "Circuit générique de commandes rapprochées pour l'électronique de puissance," PhD thesis, UGA, Grenoble, 2012.

[10] K. Loudière, "Modélisation d'une chaine d'entrainement électrique d'un point de vue CEM – Impact de la Température," PhD thesis, ECL, Lyon, 2016.